

Soliton localization in disordered one-dimensional Josephson transmission lines

S. Lomatch, E. D. Rippert, and J. B. Ketterson

Department of Physics and Astronomy, Northwestern University, Evanston, Illinois 60208

(Received 16 December 1994)

We present a study on the propagation of topological solitons (fluxons) in the strongly nonlinear system of a one-dimensional discrete Josephson transmission line with regions of disorder. Using numerical simulations, the probability of fluxon transmission is calculated stochastically, and in the presence of disorder is found to decay exponentially. The localization length is found to increase sharply with decreasing disorder strength, suggesting that fluxon-solitons may become delocalized below a certain threshold value of disorder. We describe a basic experiment to observe the predicted effects.

The Josephson transmission line (JTL) has proved to be an ideal nonlinear system in which to study soliton dynamics.¹ On the other hand, much attention has been given recently to localization effects in disordered nonlinear systems, primarily the influence of nonlinearity on the propagation characteristics of nonlinear wave packets as solitary waves.² Localization properties of solitons in a JTL are of interest since solitons in these systems can behave as ballistic particles traveling in regions of low dissipation, and have not been considered before. Conventionally, localization is a concept that generally applies to wave forms in disordered linear systems, and was first described by Anderson³ in the context of the propagation of electronic wave functions in a disordered metal. The concept was further developed by Mott and Twose,⁴ who showed that in one-dimensional electronic systems of large but finite length with a random potential only exponentially localized states occur, independent of the magnitude of the disorder or the energy of the particle. Studies of localization effects in linear classical wave systems have also received much activity, in particular, that of photon localization.⁵ The properties of extended, single-frequency waves⁶ and localized wave packets^{7,8} (solitons) in one-dimensional nonlinear systems with disorder have been discussed recently in the literature. A fundamental question in these studies has been whether nonlinearity in the presence of disorder modifies or weakens Anderson localization. The only experimental study⁹ addressing this question finds that Anderson localization is preserved, but does not consider the role of soliton excitations. Of the theoretical studies, only two^{7,8} deal directly with the effect of disorder on soliton propagation and localization. Both find that soliton localization effects either weaken⁷ (the transmission probability is modified to a power law) or vanish completely in the presence of strong nonlinearity.⁸ Neither of these systems involves topological soliton excitations, which are not necessarily expected² to behave similarly. In particular, Ref. 8 is concerned with the localization effects of envelope solitons, which are defined by their motion in the supporting nonlinear medium. Topological solitons are defined by the differences in dynamic variables between two stable states in a system with multiple stable states, and continue to exist even when their velocity is zero. Hence they

bear a closer analogy to fundamental particles, such as electrons. This work constitutes the first study that we are aware of pertaining to the localization of topological solitons, and the first physically realizable system for soliton localization of any kind.

In this paper, the system we consider is that of a one-dimensional discrete Josephson transmission line (DJTL). Both DJTL's and long-junction (continuous) JTL's support the propagation of quantized magnetic flux vortices, or fluxons, which behave as topological solitons.^{1,10,11} The spatiotemporal behavior of fluxons in a DJTL has been directly observed experimentally,¹¹ and can be accurately modeled^{12,13} by a spatially discretized partial difference form of the sine-Gordon equation with loss and bias terms [see Eq. (1)]. The continuum sine-Gordon equation is a strongly nonlinear equation which admits topological soliton (2π kink) solutions.¹⁴ Although the lossless discrete sine-Gordon equation has been shown numerically to be stable against a traveling one-soliton initial condition, the discreteness effects modify the solution to include coupling between soliton and linear modes, which is absent in the continuum limit.¹² Using the discrete sine-Gordon model, we predict numerically that when sufficient disorder is introduced into a DJTL having low dissipation, the probability of fluxon transmission decays exponentially; i.e., the fluxon-soliton becomes localized. We also compute the general behavior of the localization length as a function of system disorder strength and fluxon energy.

The simple DJTL geometry that we employ for our analysis is shown in Fig. 1. A DJTL consists of a one-dimensional (1D) array of parallel connected superconducting quantum interference device (SQUID) loops. We consider three distinct regions along the transmission line: first an injector region, on which a fluxon is induced to propagate with the application of a voltage pulse at one end and large biasing currents at each junction node; second, a steady-state region of low dissipation into which the fluxon travels; third, a disordered region, embedded in the second region. The dynamics of a propagating fluxon in the DJTL can be represented by the following second-order differential-difference equation, which is simply obtained by applying the resistively shunted junction (RSJ) model¹⁵ and Kirchhoff's laws (see Fig. 1):

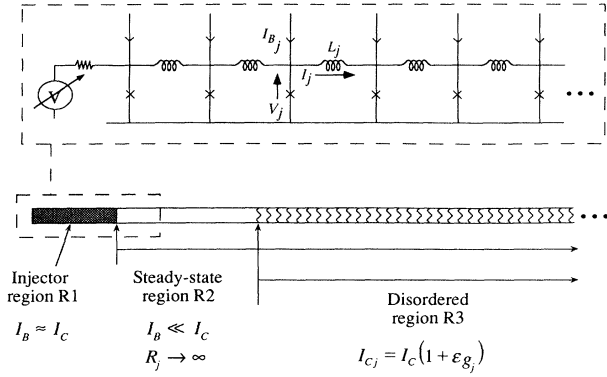


FIG. 1. Geometry of the discrete Josephson transmission line.

$$\begin{aligned}
 C_j \frac{\Phi_0}{2\pi} \frac{d^2 \phi_j}{dt^2} + \frac{\Phi_0}{2\pi R_j} \frac{d\phi_j}{dt} + I_{C_j} \sin \phi_j \\
 - \frac{\Phi_0}{2\pi L_{j-1}} (\phi_{j-1} - \phi_j) + \frac{\Phi_0}{2\pi L_j} (\phi_j - \phi_{j+1}) - I_B = 0.
 \end{aligned} \quad (1)$$

The independent variable ϕ_j is the difference between the phases of the order parameters of the superconducting layers in the j th junction, while Φ_0 ($h/2e = 2.07 \times 10^{-15}$ Wb) is the flux quantum. The first three terms on the left-hand side of Eq. (1) are three current paths in the junction: the displacement current, dissipative currents, and the tunneling supercurrent. The fourth and fifth terms reflect the inductive coupling between junctions, and the sixth term is the applied bias current. We refer to C_j , R_j , and I_{C_j} as the capacitance, shunt resistance, and critical current of the j th junction; L_j is the inductance of the j th SQUID loop. Unless specified otherwise, our parameter set for all simulations is taken to be $L \equiv L_j = 0.9$ pH, $I_C \equiv I_{C_j} = 0.42$ mA, and $C \equiv C_j = 1.1$ pF for every node j . Our choice of parameters is motivated by the geometries of DJTL's used in actual experiments.¹¹

In the injector region (R1 of Fig. 1), the junctions are overdamped ($R \equiv R_j = 1 \Omega$) for operation in the proper nonhysteretic mode, and in the presence of a Lorentz force with $I_B \sim I_C$ the induced fluxon pulse achieves a constant (steady-state) velocity. After a short propagation time the fluxon passes into R2, a region with low dissipation ($R \rightarrow \infty$), where it decelerates until it reaches a new steady-state velocity $v_s(I_B)$. In order for the fluxon to achieve a steady-state velocity v_s , a small biasing current must be applied in R2 ($I_B \ll I_C$). If $I_B = 0$ in R2, the fluxon eventually comes to rest, since it continually radiates small-amplitude linear waves¹² while in motion, and hence has a uniform drag force. In a DJTL these linear waves are in the form of oscillating loop currents in individual SQUID loops (analogous to spin waves). We have explicitly observed this type of damping in our system. The quasiparticle tunneling current in each junction is another source of dissipation, and is assumed negligible if

the operating temperature of the DJTL is well below the critical temperature of the superconductor ($T < 0.1T_C$). It is within the steady-state region (R3 of Fig. 1) that disorder is then included in our system by a random variation of the critical currents of the junctions at each node j : $I_{C_j} = I_C(1 + \epsilon g_j)$ in Eq. (1), where g_j is a Gaussian-distributed random number for which $\langle g_j \rangle = 0$ and $\langle g_j^2 \rangle - \langle g_j \rangle^2 = 1$. The strength of the applied disorder is defined by the parameter ϵ . Since the fluxon attains a velocity $v_s(I_B)$ at different times, depending on the value of I_B , the starting point of R3 varies with I_B . Once in the disordered region, the fluxon can be viewed as traveling nearly dissipationlessly through a random one-dimensional "effective" potential of the form

$$\begin{aligned}
 \mathcal{U}(\phi_j) = I_C(1 + \epsilon g_j)[1 - \cos \phi_j] \\
 + \frac{\Phi_0}{2\pi L} \left[\frac{1}{2}(\phi_j - \phi_{j-1})^2 \right. \\
 \left. + \frac{1}{2}(\phi_j - \phi_{j+1})^2 \right] - I_B \phi_j.
 \end{aligned} \quad (2)$$

It is important to note here that the fluxon-soliton is not a pointlike object, but an extended macroscopic one. A fluxon at rest spans a total of LI_C/Φ_0 (~ 5.5 for our case) junctions of the DJTL; this fluxon width is only slightly modified (decreased) by relativistic effects in this region, which are taken to be small since the steady-state velocity is a fraction of the speed of light in the DJTL. It follows that disorder in this system occurs on a scale less than the size of a fluxon. The spatial distribution of disordered sites is constant, with the junction ("lattice") spacing defining the characteristic length scale, and the disorder strength (ϵ) is variable.

When undergoing steady-state motion in the presence of disorder, we find that the fluxon has a finite probability of being nearly elastically reflected by the j' disordered site for a given random distribution $g_{j'}$. After this initial reflection, a fluxon-soliton remains trapped in the region $j < j'$.

To quantitatively measure localization effects on fluxon-solitons in our system we calculated the probability of transmission stochastically, through Monte Carlo methods. Specifically, the transmission probability distribution is given by

$$T_j^N(\epsilon, I_B) = \frac{1}{N} \sum_{k=1}^N t(\epsilon g_j^k, I_B) \quad (3)$$

for N trials, where the function $t(\epsilon g_j^k, I_B)$ is the probability of fluxon transmission (either 1 or 0) through the j th junction on the i th trial run. For each random trial, Eq. (1) is solved for the phase ϕ_j over the entire geometry shown in Fig. 1, beginning with the creation of a fluxon-soliton at one end, and continuing until an elastic reflection of the propagating fluxon occurs from the j th disordered site. Once the fluxon approaches its steady-state velocity and is near the disordered region, its motion is continuously tracked by simultaneously monitoring the phase ϕ_j and the inductor current $I_j = \Phi_0(\phi_j - \phi_{j+1})/2\pi L_j$. In particular, we detect the "collective coordinate" of the fluxon, which we define in

this discrete system as the maximum of the inductor current pulse, coincident with the center of the 2π phase kink.

Figure 2 shows the distribution of Eq. (3) calculated over a range of disorder strengths ϵ , at the biasing current value $I_B = 1.3 \mu\text{A}$. Equation (1) is solved for each event $t(\epsilon g_j^i, I_B)$ using fourth-order Runge-Kutta methods with a time step of 0.01 ps, which for our choice of model parameters is approximately equal to 1/100 the Josephson plasma period of the system. Disorder (in region R3) begins at junction $j=50$; this is close to where we estimated that fluxon had achieved a steady-state velocity. In Fig. 2 the disorder strength ϵ is expressed as a percentage, in parentheses beside each curve. The total number of events N computed for each distribution T_j is located beside the value ϵ . In general, the tails of the distributions are exponential, with a very small transient occurring near $T_j=1$. The transient becomes more prominent for increasing ϵ , and may be similar to the one observed in the transmission coefficient calculated in Ref. 8 for a nonlinear system in which envelope-soliton localization occurs. The transient in that case was attributed to the increasing influence of nonlinearity in the system. On the other hand, the transient we observe may simply be due to the fluxon-soliton having a “kinetic energy” from the injector region slightly above the steady-state value. Referring to Fig. 2, we see that for large values of ϵ ($\geq 15\%$, top graph), T_j falls off steeply from 1, and very little transmission for the fluxon-soliton is allowed beyond the point where the disorder began. As ϵ is de-

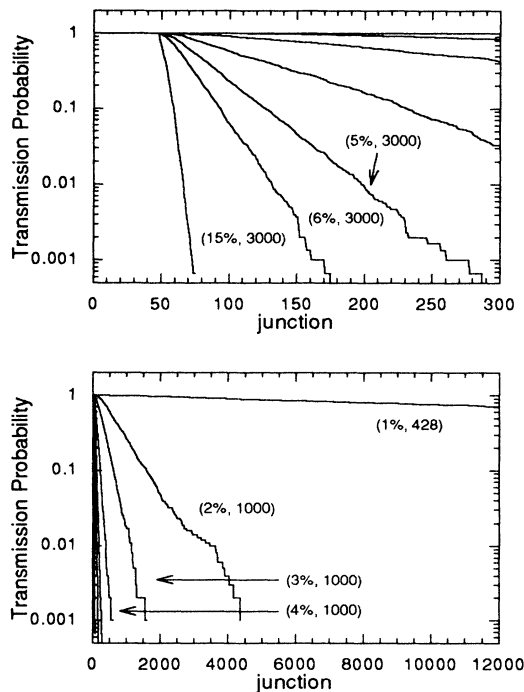


FIG. 2. Transmission probability distribution $T_j^N(\epsilon, I_B)$ as a function of junction j at $I_B = 1.3 \mu\text{A}$ for a range of disorder strengths ϵ . The bottom graph is a scaled version of the top graph.

creased (bottom graph), T_j declines more slowly from 1 at large j , and the distance over which the fluxon is transmitted with unit probability in the disordered region increases. We observe similar distributions for biasing currents two orders of magnitude below $I_B = 1.3 \mu\text{A}$.

To gauge quantitatively the rate of falloff of T_j as a function of I_B and ϵ , we assume a form

$$T_j(\epsilon, I_B) = e^{-(j-j_0)/\lambda(\epsilon, I_B)} \quad (4)$$

for the transmission probability distribution, where $\lambda(\epsilon, I_B)$ represents a localization length, and perform a two-parameter nonlinear fit to each distribution shown in Fig. 2 for j_0 and λ . The small transients are neglected in the fits. Figure 3 displays the resulting function $\lambda(\epsilon, I_B)$. We observe that the localization length approaches infinity asymptotically at small ϵ , and becomes constant (nonzero) at large ϵ . The asymptotic growth of λ at small ϵ is sharpest at lower values of I_B , and on the log-log scale of Fig. 3, the curves appear to suggest that a “mobility edge” for fluxon-soliton transmission in this 1D nonlinear system may occur at a finite value of disorder strength (ϵ_{mob}) for a given input energy (I_B). To quantify the assumption that at $\epsilon \leq \epsilon_{\text{mob}}$ the fluxon-soliton becomes delocalized and propagates without distortion, we will require further computation, preferably on a supercomputer. The present simulations took place with an optimized algorithm on HP 715 workstations; for example, the distribution contributing to the largest observed value of the localization length in Fig. 3 ($\lambda = 33\,560$ junctions at $I_B = 1.3 \mu\text{A}$ and $\epsilon = 1\%$) required over 1 month of integration time on several machines, yielding only 428 events.

We have noted that the spatial width of the fluxon-soliton is fixed in our system for all simulations, and is larger than the spacing of disordered sites (5.5:1 ratio). The effect of fluxon width on the transmission properties of the fluxon through disorder was briefly investigated. The flux quantization condition implies that the fluxon width becomes larger with decreasing SQUID loop inductance L_j . If we decrease L_j in the DJTL by a factor of 2 (approximately doubling the width), and change the capacitance and injector resistance to keep the speed of the injected fluxon the same (so that only the fluxon “mass” is increased), we find that fluxon transmission is

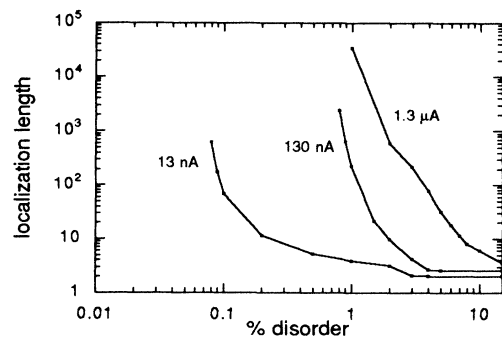


FIG. 3. Fitted localization length $\lambda(\epsilon, I_B)$ as a function of disorder strength ϵ for a range of biasing currents I_B .

greatly enhanced. Indeed, at $\varepsilon = 5\%$ for $I_B = 1.3 \mu\text{A}$, the fluxon travels with unit probability ~ 34 times longer, and the subsequent localization length is ~ 12 times greater. A decrease in the fluxon width by a similar amount does not allow the fluxon to have a sufficient kinetic energy to propagate past the injector region.

While the focus of this paper has been on the theoretical analysis of fluxon-solitons in a disordered DJTL to quantify localization effects, we would like to comment on a possible experimental implementation. One could fabricate a DJTL with an overdamped, high-bias injector region and an underdamped, low-bias steady-state region. Both overdamped¹¹ and underdamped¹⁶ DJTL's have been fabricated to study fluxon-soliton dynamics. The disorder in the DJTL is realized by exposing an appropriate length of the steady-state region to a radiation source (i.e., x rays, γ rays, or α particles). There are numerous experimental groups around the world who are already routinely performing experiments in the detection of soft x rays, α particles, neutrinos, and dark matter using superconducting tunnel junctions.¹⁷ Control of the energy¹⁸ and dosage¹⁹ of soft x-ray irradiation has been achieved as has controlled irradiation using the electron beam in a scanning electron microscope (SEM) with a liquid-helium-cooled sample stage.²⁰ Columnation of soft x rays into localized, movable spots with diameters as small as $5 \mu\text{m}$ have also been achieved,²¹ and electron irradiation via SEM can be focused into a movable 100 \AA diameter spot.²⁰ The breaking of Cooper pairs and subsequent production of quasiparticles in the individual tunnel-junction electrodes would perturb the critical currents in these junctions. The effect of quasiparticles produced in an x-ray-absorption event on the superconducting energy gap has been considered in some detail in the literature.²² Critical current suppression in Josephson junctions in a DJTL due to x-ray absorption has also been discussed.²³ The effective lifetime of such excitation events is on the order of microseconds due to phonon

trapping effects.²⁴ The source activity should be chosen so that each junction undergoes an absorption event once every few relaxation periods. One then injects a fluxon into the injector and detects it at the end of the disordered region, using standard single-flux-quantum (SFQ) electronics²⁵ (dc-SFQ and SFQ-dc converters). The ratio of detected fluxons to injected fluxons would be a direct measure of the transmission coefficient. Parameter variations in typical superconducting electronics foundries is around $3\sigma = 5-10\%$, and therefore an appropriate bias current should be chosen so that measurable fluxon localization occurs at higher disorder strengths. Perturbations due to phonons from substrate absorption events and dissipation due to tunneling of excited quasiparticles should also be taken into account. Methods for decoupling of junctions from substrate phonons using a base electrode trapping layer,²⁶ back etching of the substrate,²⁰ and Bragg mirrors²⁷ are discussed in the literature. In addition, a localized fluxon will not dissipate in the DJTL and should be removed before the next injection by pulsing the bias current to a high enough value to delocalize it.

In summary, we have demonstrated through dynamic numerical simulation that fluxon-solitons localize in a disordered 1D discrete Josephson transmission line with low dissipation. The stochastically calculated transmission probability distribution as a function of disorder strength and fluxon energy is exponential; the resulting localization length asymptotically increases at small, but finite, disorder strength, suggesting that the fluxon delocalizes below a threshold value of this strength. That we are aware of, this work constitutes the first such study of the localization properties of topological solitons. The localization effects of disorder on fluxon-solitons that we calculate in this 1D system should be observable in a real experimental implementation; we have given brief specifications for such an implementation.

¹T. A. Fulton, R. C. Dynes, and P. W. Anderson, Proc. IEEE **61**, 28 (1973); A. C. Scott, F. Y. F. Chu, and S. A. Reible, J. Appl. Phys. **47**, 3272 (1976).

²S. A. Gredekskul and Yu. S. Kivshar, Phys. Rep. **216**, 1 (1992), and references therein.

³P. W. Anderson, Phys. Rev. **109**, 1492 (1958).

⁴N. F. Mott and W. D. Twose, Adv. Phys. **10**, 107 (1961).

⁵See, for example, *Scattering and Localization of Classical Waves in Random Media*, edited by P. Sheng (World Scientific, Singapore, 1990).

⁶B. Doucot and R. Rammal, Europhys. Lett. **3**, 969 (1987).

⁷Q. Li, C. M. Soukoulis, St. Pnevmatikos, and E. N. Economou, Phys. Rev. B **38**, 11 888 (1988).

⁸Yu. S. Kivshar, S. A. Gredekskul, A. Sánchez, and L. Vázquez, Phys. Rev. Lett. **64**, 1693 (1990).

⁹M. J. McKenna, R. L. Stanley, and J. D. Maynard, Phys. Rev. Lett. **69**, 1807 (1992).

¹⁰A. Matsuda and T. Kawakami, Phys. Rev. Lett. **51**, 694 (1983).

¹¹A. Fujimaki, K. Nakajima, and Y. Sawada, J. Appl. Phys. **61**,

5471 (1987); Phys. Rev. Lett. **59**, 2895 (1987).

¹²J. F. Currie, S. E. Trullinger, A. R. Bishop, and J. A. Krumhansl, Phys. Rev. B **15**, 5567 (1977).

¹³K. Nakajima and Y. Onodera, J. Appl. Phys. **49**, 2958 (1978).

¹⁴A. C. Scott, F. Y. F. Chu, and D. W. McLaughlin, Proc. IEEE **61**, 1443 (1973).

¹⁵A. Barone and G. Paterno, *Physics and Applications of the Josephson Effect* (Wiley, New York, 1982).

¹⁶H. S. J. van der Zant, E. H. Visscher, D. R. Curd, T. P. Orlando, and K. A. Delin, IEEE Trans. Appl. Supercond. **3**, 2658 (1993).

¹⁷See, for example, *Proceedings of the Fifth International Conference on Low Temperature Detectors* [J. Low Temp. Phys. **93**, 185 (1993)].

¹⁸S. E. Labov, L. H. Hiller, C. A. Mears, M. Frank, H. Netel, F. Azgui, and A. T. Barfknecht, IEEE Trans. Appl. Supercond. (to be published).

¹⁹N. Rando, A. Peacock, A. van Dordrecht, R. Engelhardt, C. Foden, B. G. Taylor, P. Garé, J. Lumley, and C. Pereira, Nucl. Instrum. Methods Phys. Res. Sect. A **313**, 173 (1992).

- ²⁰S. Lemke, F. Hebrank, R. Gross, R. P. Huebener, Th. Weimann, R. Pöpel, J. Niemeyer, U. Schnakenberg, and W. Benecke, in *ESA Symposium on Photon Detectors for Space Instrumentation*, edited by T. D. Guyenne and J. J. Hunt, ESA Publication No. ESA SP-356 (ESA, Neuilly-sur-Seine, 1992), p. 335.
- ²¹P. Verhoeve, N. Rando, P. Videler, A. Peacock, A. van Dordrecht, D. J. Goldie, J. M. Lumley, J. Howlett, M. Wallis, and R. Venn, *Proc. SPIE* **2283**, 172 (1994).
- ²²D. Van Vechten and K. S. Wood, *Phys. Rev. B* **43**, 12 852 (1991).
- ²³E. D. Rippert, S. Lomatch, J. B. Ketterson, S. N. Song, H. C. Wang, and S. R. Maglic, *J. Low Temp. Phys.* **93**, 665 (1993).
- ²⁴A. Rothwarf and B. N. Taylor, *Phys. Rev. Lett.* **19**, 27 (1967).
- ²⁵K. K. Likharev and V. K. Semenov, *IEEE Trans. Appl. Supercond.* **1**, 3 (1991).
- ²⁶C. L. Foden, N. Rando, A. Peacock, and A. van Dordrecht, *J. Appl. Phys.* **74**, 6774 (1993).
- ²⁷E. D. Rippert, J. B. Ketterson, J. Chen, S. N. Song, S. Lomatch, S. R. Maglic, C. Thomas, M. A. Chieda, and M. P. Ulmer, *Proc. SPIE* **1743**, 12 (1992).